Journal of Colloid and Interface Science **244,** 303–312 (2001)
doi:10.1006/jcis.2001.7944, available online at http://www.idealibrary.com on IDEAL®

Long-Scale Evolution of Thin Liquid Films Bounded by a Viscous Phase with Diffusing Charged Surfactants

Elias Ramos-de-Souza,*[,1] Celia Anteneodo,† Dominique Gallez,‡ and Paulo Mascarello Bisch†

*Departamento de Ciências Aplicadas, Centro Federal de Educação Tecnológica da Bahia, Rua Emídio Santos, s/n, 40300-010 Salvador-BA, Brazil; †Instituto de Biofísica Carlos Chagas Filho, Universidade Federal do Rio de Janeiro, CCS, S026, Cidade Universitária, Ilha do Fundão 21949-900 Rio de Janeiro, Brazil; and ‡Service de Chimie Physique and Centre for Nonlinear Phenomena and Complex Systems, CP 231, Université Libre de Bruxelles, Blvd. du Triomphe, 1050 Brussels, Belgium

Received July 17, 2000; accepted September 3, 2001; published online November 9, 2001

The long-scale evolution of a thin liquid film between a viscous bounding phase and a fixed substrate is addressed. Positively charged surfactants are allowed to diffuse along the free water/bounding-phase interface and the substrate has fixed electric charges of opposite sign. We assume that the free surface deformation occurs on a length scale that far exceeds the film thickness. In that case, the Navier–Stokes and continuity equations with appropriate boundary conditions lead to a system of two nonlinear coupled equations, for the film thickness and for the concentration of the diffusing charged surfactant. The direction of Marangoni flows depends on the relationship between the viscosities of the film and of the bounding phase. Because the surfactants are electrically charged, the film dynamics accounts for the competition between diffusive flux and ion migration. The numerical integration of the coupled equations makes it possible to follow the time evolution of the film subject to an initial random perturbation. Numerical results are compatible with linear analysis calculations. The model predicts the formation of steady patterns both for the film thickness and for the distribution of the charged surfactant. © 2001 Elsevier Science

Key Words: **thin liquid films; electrohydrodynamics; morphological patterns; phase separation; Marangoni effect.**

INTRODUCTION

Thin liquid films are ubiquitous structures of scientific and technological importance in a variety of applications. They appear, for example, in coatings and dewetting phenomena, in paints, in adhesives, and in photographic films. In biological systems they appear as lipid films, aqueous films lining the mammalian lungs, tear films in the eyes, and aqueous layers in cell adhesion, among other examples.

The general subject of the long-scale evolution of thin liquid films was recently reviewed by Oron *et al.* (1). These films exhibit a variety of spatiotemporal instabilities leading to either rupture or formation of steady-state patterns. In particular, pattern formation appears as a morphological phase separation phenomenon where the film thickness shows stable periodic shapes (morphological patterns). In the past decade some progress has been made on the description of pattern formation in thin liquid films since such a concept appeared (2). By numerical analysis, morphological patterns were demonstrated in 2D thin films subjected to antagonistic forces (3–7). An analytical proof of pattern formation in 2D thin aqueous films delimited by a fixed substrate and a gaseous phase with constant tension was given (8): morphological patterns become possible whenever there is a competition between external attractive and repulsive forces. The crucial role of antagonistic forces on the formation of such patterns was also confirmed for the case of 3D thin liquid films (9, 10).

Also, some efforts have been made to describe the role of surface active materials on the long-scale evolution of thin films. The influence of insoluble neutral surfactants in the water–gas interface on the formation of patterns was investigated (11). Neutral surfactants do not essentially alter the resulting film thickness profile but just the time required for pattern building. In this case, when the steady pattern is established, the surfactant distribution is uniform, despite transient inhomogeneities.

However, the models considered until now do not account for the viscosity of the bounding phase. Although that is a good approximation for the case of an aqueous film bounded by a gaseous phase, it is no longer valid for the cases in which a relatively viscous bounding phase is present. In particular, thin liquid films bounded by viscous layers are typical in biological processes like cell adhesion, where thin aqueous films are bounded by membranes. The adhesion of cells or vesicles on fixed substrates like supported membranes has been the subject of recent studies (12). Due to the interplay of nonspecific forces, interesting steady patterns on adhesion of cells and vesicles can arise. Red blood cells suspended in a solution with adhesive macromolecules adhere to each other and show spatially periodic contact points with lateral distance of the order of 1 μm (13, 14). Pattern formation can also result from the competition between capillary, (repulsive) electrostatic, and (attractive) macromolecular depletion or cross-bridge forces (13, 15). The competition between attractive van der Waals forces and

[1] To whom correspondence should be addressed. Fax: 55 71 242 0621. E-mail: eramos@cefetba.br.

0021-9797/01 $35.00
© 2001 Elsevier Science
All rights reserved

repulsive hydration and/or electrostatic forces may also lead to spatially periodic steady patterns in vesicles (15). Blistering on giant charged vesicles, driven by electrostatic effects due to their interaction with a substrate bearing opposite charge, was also observed (16, 17). Hemifusion of lipid vesicles has been observed by fluorescence video microscopy showing that, in one of several different possible scenarios, two adherent vesicles can pass from a flat contact to a point contact (18).

Also, cell biomembranes include charged molecules and are immersed in aqueous media where salt ions are dispersed, therefore, electrostatic interactions are expected to play a crucial role and should be considered in any realistic model. Within this picture, we model here a thin aqueous film between a fixed charged substrate and a fluid bounding phase with insoluble charged surfactants on the water/bounding-phase interface. Both the film and the bounding layer are viscous fluid phases. The ionic strength of the aqueous film is also taken into account. We also consider that the substrate and the surfactants have opposite electric charges. This situation leads to a simple model where the electric disjoining pressure derived by Parsegian and Gingell (19), following the Debye–Hückel theory, has attractive and repulsive contributions and then considers the underlying physics of the problem treated in this paper.

Within this model we obtain a system of two nonlinear coupled equations for the film thickness and for the concentration of insoluble surfactants. By considering the viscosity of the bounding phase we find new features concerning the Marangoni convection. If the viscosity of the bounding phase is greater than that of the film phase the direction of the Marangoni flows is reversed with respect to the case of a film bounded by a nonviscous gas phase. Also, because the diffusing surfactant molecules on the water/bounding-phase interface are electrically charged there is an electrochemical diffusion term in the evolution equation for the surfactant concentration rather than a purely chemical one as considered before (20, 11). The presence of electrically charged surfactants leads to a new outcome concerning pattern formation in thin liquid films. Besides patterns for the film thickness (morphological patterns), steady patterns for the surfactant concentration (phase separation) also arise.

FORMULATION

Consider a thin aqueous layer of mean thickness $\bar{h}_0$, density $\bar{\rho}$, and viscosity $\bar{\mu}$, bounded by a fixed substrate and a fluid bounding phase of density $\bar{\rho}'$ and viscosity $\bar{\mu}'$ (Fig. 1). The thin aqueous layer will be modeled as a thin liquid film sandwiched between a water/substrate and a water/bounding-phase interface. The film thickness $\bar{h}(\bar{x}, \bar{t})$ is a function of lateral coordinate $\bar{x}$ and time $\bar{t}$. We neglect inhomogeneities in the $\bar{y}$ direction. The free surface separates the aqueous film from the bounding phase and is located at $\bar{z} = \bar{h}(\bar{x}, \bar{t})$, where $\bar{z}$ is the transverse coordinate. It represents an interface where charged surfactant (lipid) molecules are free to move with a lateral diffusion coefficient $\bar{D}$. The substrate bears opposite electric charge and is located at $\bar{z} = 0$.

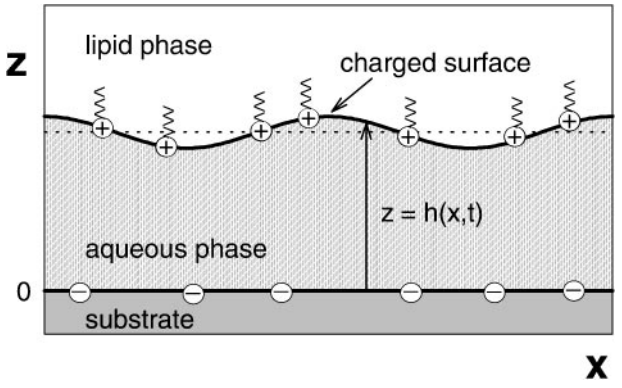

FIG. 1. The system: a thin aqueous film is bounded by a fixed substrate and by a free surface which delimits a lipid phase. The substrate and the free surface have electric charge densities of opposite sign (σ_s and σ, respectively). The free surface is described by $z = h(x, t)$.

The 2Dimensional motion inside the film is governed by Navier–Stokes equations. We consider the possibility of a conservative body force with potential Φ on the fluid as well as external normal $\bar{\Pi}$ and tangential $\bar{\tau}$ stresses on the interfaces (1). The free surface possesses surface properties like surface tension, mass, and charge densities. Consequently, if the diffusing surfactant has surface concentration $\bar{\Gamma}(\bar{x}, \bar{t}) = \bar{\sigma}(\bar{x}, \bar{t})/\bar{Z}$, where $\bar{Z}$ is the molar charge and $\bar{\sigma}(\bar{x}, \bar{t})$ is the surface charge concentration, the surface tension $\bar{\Sigma}(\bar{\Gamma})$ will vary according to the local surfactant concentration due to solutal Marangoni effect (21). In addition, a conservation equation is adopted for the charged lipid concentration where $\bar{\sigma}(\bar{x}, \bar{t})$ varies in time due to convection and diffusion effects (20). Here, we have electrochemical diffusion rather than the purely chemical one as considered before (11). The surface curvature will be considered to be so large that the rate of change of $\bar{\sigma}(\bar{x}, \bar{t})$ due to dilatation of the surface is neglected. The equations of motion as well as the corresponding boundary conditions at the free surface are considerably simplified whenever the film deformation occurs on a length scale that far exceeds the film thickness (22). A system of two coupled nonlinear evolution equations for a thin film bounded by a nonviscous gas phase on a solid substrate with neutral insoluble surfactants, resulting from a long wavelength reduction procedure (1), was already given (20). Here we extend that model for a thin film bounded by a viscous phase with electrically charged insoluble surfactants (see Appendix). Then we obtain the following equations for the dimensionless film thickness h and for the dimensionless surface charge concentration σ:

$$
\begin{aligned}
h_t &= \left[\frac{\tilde{M}}{2\mu_d} h^2 \sigma_x - \frac{\Sigma_0}{3} h^3 h_{xxx} - \frac{1}{3} h^3 \phi_x \right]_x, \\
\sigma_t &= \left[D(\sigma_x + \tilde{Z}\sigma\psi_x) + \frac{\tilde{M}}{\mu_d} h\sigma\sigma_x \right. \\
&\qquad \left. - \frac{\Sigma_0}{2} h^2 \sigma h_{xxx} - \frac{1}{2} h^2 \sigma \phi_x \right]_x,
\end{aligned}
\qquad [1]
$$

where subscripts t and x denote differentiation. The dimensionless quantities $h = \bar{h}/\bar{h}_0$, $x = \bar{x}/\bar{h}_0$, $z = \bar{z}/\bar{h}_0$, $t = \bar{v}\bar{t}/\bar{h}_0^2$, and $\sigma = (\bar{h}_0^2/\bar{\rho}\bar{\nu}^2)^{1/2}\,\bar{\sigma}$ are, respectively, the dimensionless film thickness, lateral coordinate, normal coordinate, time, and surfactant charge concentration, $\bar{\nu} = \bar{\mu}/\bar{\rho}$ being the kinematic viscosity. $D = \bar{D}/\bar{\nu}$, $\tilde{Z} = (\bar{\rho}\bar{\nu}^2)^{1/2}\bar{Z}/(\bar{R}\bar{T})$, where $\bar{R}$ is the gas constant and $\bar{T}$ is the absolute temperature. The dimensionless surface tension $\Sigma = (\bar{h}_0/\bar{\rho}\bar{\nu}^2)\bar{\Sigma}$ is considered to satisfy the linear equation of state,

$$\Sigma = \Sigma_0 - \tilde{M}\sigma, \qquad [2]$$

where $\tilde{M} = -\partial\Sigma/\partial\sigma$ is the (constant) reduced Marangoni number, and Σ_0 is the (dimensionless) surface tension at equilibrium. The contribution of uncharged surfactant molecules to the surface tension are already included in Σ_0, since we are assuming that variations of Σ are due to charged surfactants only. Here the viscosity of the bounding phase μ' is taken into account on the film evolution through $\mu_d = 1 - \mu'/\mu$. For $\mu' > \mu$, the Marangoni term in the evolution equations [1] has opposite sign with respect to the case of a water–gas interface (20) in which the gas viscosity is neglected.

In Eqs. [1] the potential function $\phi = (\bar{h}_0^2/\bar{\rho}\bar{\nu}^2)\bar{\phi}$ is the dimensionless form of the disjoining pressure ϕ, the difference between the pressure inside the film and the bulk forming film phase and adjacent membrane phase pressures. The DLVO Theory (23) accounts for interaction of charged particles in electrolyte solutions. We will consider that the only operative forces on the film interfaces come from electrostatic effects in the aqueous phase. The electric disjoining pressure for surfaces with charges of the same sign is always repulsive (24). Here, where surfaces charges have opposite signs, the disjoining pressure will contain both attractive and repulsive terms (19). According to the results derived by Parsegian and Gingell (19), the body forcing tangential stress is $\tau = 0$ and the disjoining pressure ϕ accounts for the external electrical force in the aqueous phase and for the normal electric stress, i.e., $\phi = \Phi - \Pi$ (see Appendix, Eq. [A-5]) and is given by

$$\phi(h,\sigma) = \left(\frac{8\pi}{\epsilon}\right)\frac{\sigma^2 + \sigma\sigma_s(e^{\kappa h} + e^{-\kappa h}) + \sigma_s^2}{(e^{\kappa h} - e^{-\kappa h})^2}, \qquad [3]$$

where ϵ is the film phase dielectric constant, $\kappa = \bar{h}_0\bar{\kappa}$ is the (dimensionless) inverse of the Debye length, and $\sigma_s = (\bar{h}_0^2/\bar{\rho}\bar{\nu}^2)^{1/2}\,\bar{\sigma}_s$ is the (dimensionless) charge density on the substrate.

The potential $\psi = (\bar{\rho}\bar{\nu}^2)^{-1/2}\bar{\psi}$ accounts for the electric surface potential on the free surface and reads

$$\psi(h,\sigma) = \left(\frac{4\pi}{\epsilon\kappa}\right)\frac{2\sigma_s + \sigma(e^{\kappa h} + e^{-\kappa h})}{e^{\kappa h} - e^{-\kappa h}}. \qquad [4]$$

$\bar{\phi}$ and $\bar{\psi}$ were obtained at the low surface potential approximation and hold for $\bar{\psi} \le 25$ mV at $T = 25^\circ$C. It was shown (19) that when ions are excluded from the regions behind the interacting surfaces repulsion between charged surfaces of opposite sign may occur. But surfaces bearing charges of the same sign never attract one another. For the case considered here, i.e., charged surfaces of opposite sign ($\sigma > 0$ and $\sigma_s < 0$), the dependence of the disjoining pressure ϕ (Eq. [3]) on the film thickness h is shown in Fig. 2a for different values of the free surface charge. Note that if $\sigma \neq -\sigma_s$, ϕ will be either negative (the surfaces attract one another) or positive (the surfaces repel one another), depending on the distance between the substrate and the free surface. However, if $\sigma = -\sigma_s$ there will be always attraction. Charged surfaces of opposite sign can repel each other because the condition confining the ionic double layer to the finite region of thickness h acts to increase the osmotic pressure in the region $0 \le z \le h$. The dependence of the free surface electric potential ψ on h, for different values of the surface charges, is shown in Fig. 2b. ψ will never be negative for $\sigma \le -\sigma_s$. However, if $\sigma > -\sigma_s$, ψ will change from positive to negative values as the film thickness h decreases.

The long wavelength approximation is carried out by supposing that the wavelength of the film deformation λ is far

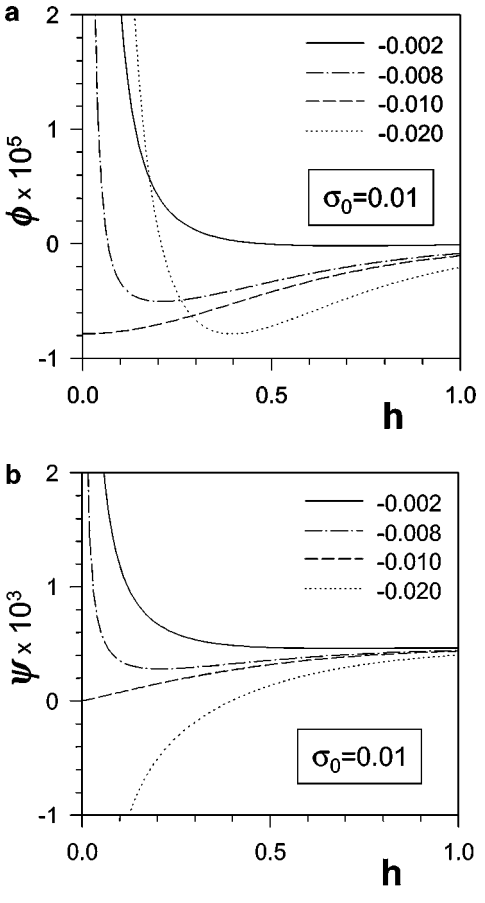

FIG. 2. Potentials of the operative forces. (a) Disjoining pressure ϕ (Eq. [3]) and (b) electric surface potential ψ (Eq. [4]), as a function of the film thickness h for different values of the electric charge density σ_s of the substrate (indicated on the figure) and charge density of the vesicle $\sigma_0 = 0.01(\kappa = 10/3)$.

TABLE 1
Reference Values of the Film Parameters

Parameter	Symbol	Reference value
Film viscosity	$\bar{\mu}$	10^{-2} g/cm s
Membrane viscosity	$\bar{\mu}'$	10^{-1} g/cm s
Film density	$\bar{\rho}$	1 g/cm^3
Kinematic viscosity	$\bar{\nu}$	10^{-2} cm^2/s
Equilibrium film thickness	$\bar{h}_0$	10^{-6} cm
Surface diffusion coefficient	$\bar{D}$	10^{-7} cm^2/s
Free surface charge at equilibrium	$\bar{\sigma}_0$	5×10^2 ues/cm^2
Support charge density	$\bar{\sigma}_s$	-6×10^2 ues/cm^2
Molar charge concentration	$\bar{Z}$	3×10^{14} ues/mol
Molar thermal energy	$\bar{R}\bar{T}$	2.4×10^{10} erg/mol
Inverse of Debye length	$\bar{\kappa}$	3.3×10^7 cm^{-1}
Equilibrium surface tension	$\bar{\Sigma}_0$	10^{-2} dyn/cm
Marangoni number	$\bar{M}$	3×10^9 erg/mol
Dimensionless film parameters		
Viscosity difference	$\mu_d = (1 - \bar{\mu}'/\bar{\mu})$	-10
Equilibrium film thickness	$h_0 = \bar{h}_0/\bar{h}_0$	1
Surface diffusion coefficient	$D = \bar{D}/\bar{\nu}$	10^{-5}
Free surface charge at equilibrium	$\sigma_0 = (\bar{h}_0^2/\bar{\rho}\,\bar{\nu}^2)^{1/2}\bar{\sigma}_0$	5×10^{-2}
Support charge density	$\sigma_s = (\bar{h}_0^2/\bar{\rho}\,\bar{\nu}^2)^{1/2}\bar{\sigma}_s$	-6×10^{-2}
Charge concentration over thermal energy	$\tilde{Z} = (\bar{\rho}\,\bar{\nu}^2)^{1/2}\bar{Z}/(\bar{R}\,\bar{T})$	1.2×10^2
Inverse of Debye length	$\kappa = \bar{h}_0\bar{\kappa}$	3.3
Surface tension	$\Sigma_0 = (\bar{h}_0/\bar{\rho}\,\bar{\nu}^2)\bar{\Sigma}_0$	10^{-4}
Reduced Marangoni number	$\tilde{M} = (\bar{\rho}\,\bar{\nu}^2)^{-1/2}\bar{M}/\bar{Z}$	10^{-3}

greater than the film thickness h. A small parameter $\eta = h/\lambda \ll 1$ is defined and all of the variables and parameters of the basic equations are scaled on it. Keeping the lower order terms in η allows to obtain simplified equations. The evolution Eqs. (1) were obtained by assuming that the dimensionless variables are $x = \mathcal{O}(\eta^1)$, $z = \mathcal{O}(1)$, $t = \mathcal{O}(\eta^n)$, $h = \mathcal{O}(1)$, and as a result the order of magnitude for the film parameters are $\phi = \mathcal{O}(\eta^{2-n})$, $\Sigma_0 = \mathcal{O}(\eta^{4-n})$, $\mu_d^{-1}\tilde{M} = \mathcal{O}(\eta^{1-n/2})$, σ, $\sigma_s = \mathcal{O}(\eta^{1-n/2})$, and $D = \mathcal{O}(\eta^{2-n})$.

The choice of n is related to the diffusion time scale. Although the evolution equations are independent of the particular choice of n, n does determine the order of magnitude of the parameters in the equations. Note that higher values of n lead to lower tension and lower diffusion coefficient, for instance. For illustration, Table 1 displays a set of realistic values of parameters chosen do give some qualitative correspondence with the experiments carried out by Nardi *et al.* (16) on the adhesion of a giant vesicle to a supported membrane, which match well with $n = 5$.

LINEAR ANALYSIS

We suppose that the film is initially homogeneous and that model [1] admits a family of steady-state solutions. In what follows, we analyze the stability of the steady-state solution $(h, \sigma) = (1, \sigma_0)$ corresponding to a plane film with homogeneous charge concentration σ_0 on the free surface. We introduce the small deviations $h'(x,t) = h(x,t) - 1$ and $\sigma'(x,t) = \sigma(x,t) - \sigma_0$ from the steady state into Eqs. [1] and obtain a linearized problem which, in a system with periodic boundary conditions on a bounded domain $0 \le x \le L$, admits solutions of the form

$$\begin{pmatrix} h' \\ \sigma' \end{pmatrix} = \begin{pmatrix} \alpha \\ \beta \end{pmatrix} \exp(wt + ikx), \qquad [5]$$

where w is the growth rate of the disturbance and k is its wavenumber. The eigenvalue problem,

$$w \begin{pmatrix} \alpha \\ \beta \end{pmatrix} = k^2 \begin{pmatrix} \ell_{11} & \ell_{12} \\ \ell_{21} & \ell_{22} \end{pmatrix} \begin{pmatrix} \alpha \\ \beta \end{pmatrix}, \qquad [6]$$

where,

$$\begin{aligned} \ell_{11} &= \frac{1}{3}(\phi_h' - \Sigma_0 k^2), \\ \ell_{12} &= -\frac{1}{2}\mu_d^{-1}\tilde{M} + \frac{1}{3}\phi_h', \\ \ell_{21} &= \sigma_0\left(-D\tilde{Z}\psi_h' + \frac{1}{2}\phi_h' - \frac{\Sigma_0}{2}k^2\right), \\ \ell_{22} &= -D(1 + \sigma_0\tilde{Z}\psi_\sigma') - \mu_d^{-1}\tilde{M}\sigma_0 + \frac{\sigma_0}{2}\phi_\sigma', \end{aligned} \qquad [7]$$

and

$$\begin{aligned} \phi_h' &= \left(\frac{\partial\phi}{\partial h}\right)_{(1,\sigma_0)} = -\frac{8\pi\kappa}{\epsilon}\left[2\left(\sigma_0^2 + \sigma_s^2\right)e^{-2\kappa} + \sigma_0\sigma_s e^{-\kappa}\right], \\ \phi_\sigma' &= \left(\frac{\partial\phi}{\partial\sigma}\right)_{(1,\sigma_0)} = \frac{8\pi}{\epsilon}e^{-2\kappa}(2\sigma_0 + \sigma_s e^{\kappa}), \\ \psi_h' &= \left(\frac{\partial\psi}{\partial h}\right)_{(1,\sigma_0)} = -\frac{8\pi}{\epsilon}\sigma_s e^{-\kappa}, \\ \psi_\sigma' &= \left(\frac{\partial\psi}{\partial\sigma}\right)_{(1,\sigma_0)} = \frac{4\pi}{\epsilon\kappa} \end{aligned} \qquad [8]$$

is then obtained, leads to the characteristic equation:

$$w^2 - k^2(\ell_{11} + \ell_{22})w + k^4(\ell_{11}\ell_{22} - \ell_{12}\ell_{21}) = 0. \qquad [9]$$

For values of the parameters of the order of those indicated in Table 1, the characteristic Eq. [9] has two real roots. One of them, w_1, is always negative, whereas the other one, w_2, has not a definite sign. The system will be asymptotically stable if $w_2 < 0$ or unstable if $w_2 > 0$, while marginal stability corresponds to $w_2 = 0$. The critical wavenumber, k_c, for which $w_2 = 0$, satisfies

$$k_c^2 = \frac{\phi_h' + Q}{\Sigma_0}, \qquad [10]$$

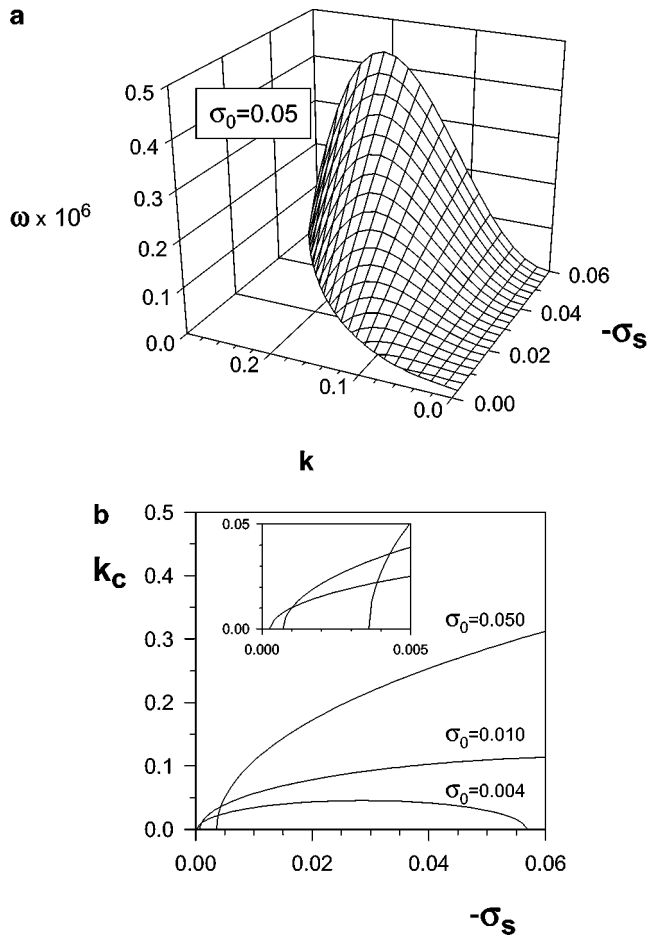

FIG. 3. Linear analysis. (a) Growth rate of the disturbance ω as a function of the wavenumber k and the electric charge density of the substrate σ_s. Charge density of the vesicle at equilibrium is $\sigma_0 = 0.05$. (b) Critical wavenumber k_c for which $\omega = 0$ as a function of σ_s and different values of $\sigma_0 \cdot \mu_d = -10$, $\tilde{M} = 10^{-3}$, $\Sigma_0 = 10^{-3}$, $D = 10^{-5}$, and $\kappa = 10/3$. (Inset) Enlargement of the plot close to the origin of coordinates. $-\sigma_{s,c}$ increases almost linearly with σ_0.

with

$$Q = 2D\tilde{Z}\sigma_0\psi_h' \frac{3\tilde{M} - 2\mu_d\phi_\sigma'}{\tilde{M}\sigma_0 + 4\mu_d D(1 + \tilde{Z}\sigma_0\psi_\sigma')}. \qquad [11]$$

It was shown (20) that in an uncharged film with one species of surfactant molecules the critical wavenumber depends only on tension and on the derivative with respect to h of the disjoining pressure. Here, because of the competition between diffusion and charge migration, k_c depends also on the diffusion coefficient and on the Marangoni number, through Q. We will discuss some consequences of this new feature on the evolution of the disturbances by solving numerically the full nonlinear evolution Eqs. [1].

Equation [10] shows that several film parameters could play the role of a control (bifurcation) parameter in the sense they have a critical value in which the behavior of the system changes qualitatively from stability to instability. Nardi *et al.* (16) regarded the support charge as a control parameter in adhesion between a giant vesicle and a support of oppositely charged surfaces. On Fig. 3 we resume the result of the linear analysis on our model taking σ_s as a control parameter. Figure 3a shows that increasing σ_s increases both the growth rate of the perturbation and k_c (decreases the wavelength) for a range of relatively samaller values of σ_s and that k_c will rather decrease with σ_s for higher values of the "support charge" (Fig. 3b). One can also see on Fig. 3b that there is a σ_0-dependent cutoff on the curve k_c vs σ_s. It means that for each fixed value of the membrane charge σ_0 there is a minimum value of $-\sigma_s$ ($-\sigma_{s,c}$) for the instabilities to appear. This threshold value increases almost linearly with the surfactant charge concentration σ_0, resulting in $-\sigma_{s,c} \ll \sigma_0$.

NUMERICAL RESULTS

We follow basically the same numerical methodology employed previously (7). Equation [1] is solved as an initial value problem considering spatially periodic boundary conditions (PBC). This type of boundary conditions allows to investigate the behavior of a film whose thickness is small compared to its length which corresponds to our case. Through the linear analysis, the critical wavelength λ_c ($\lambda_c = 2\pi/k_c$) can be estimated. Then, the bounded domain with PBC is taken as $0 \le x \le L$, where L is chosen arbitrarily just requiring that $L > \lambda_c$.

We consider random initial values for the thickness of the film. For the vesicle charge density we consider a uniform initial value, but random initial values, similarly as for the film thickness, lead essentially to the same results.

We use finite difference methods to solve Eq. [1], by means of a FTCS scheme (25). An explicit scheme is applied for the time derivative and centered staggered differences in space are used to obtain the successive derivatives with respect to x. Thereafter, the finite-difference representation of Eq. [1] is solved iteratively until a stable shape is observed.

By means of this numerical procedure we are able to follow the evolution of the perturbed film. The shape of the film surface as well as the surface charge density profile, obtained from numerical integration, as a function of x at various times t are represented in Figs. 4a and 4b. Figure 4c shows the temporal behavior of the minimal values of $h(x, t)$ and $\sigma(x, t)$ followed for controlling the stability of the profiles. Notice that here also the surfactant concentration reaches a steady nonhomogeneous pattern due to the presence of electrochemical diffusion.

The perturbation rapidly tunes the fastest growth mode whose characteristic wavelength is somewhat greater than the critical wavelength (see Fig. 3b). Numerical integration shows that Eqs. [1] indeed admit several steady solutions (Fig. 4a). Observe the temporal behavior of the minimal and the maximal values of $h(x, t)$ in Fig. 5b. Various "metastable" patterns appear as time goes by. The surface charge concentration evolves in a similar way.

The linear analysis predicts that the critical wavenumber k_c presents a maximal value for a given σ_s (see Fig. 3b, for

$\sigma_0 = 0.004$). In fact, numerical integration results are consistent with this linear prediction (see Fig. 6a). As $-\sigma_s$ increases, the wavelength first decreases (three first frames) and then increases (last frame). Numerical integration also confirms that the uniform profile is stable below a critical value of σ_s (Fig. 6b).

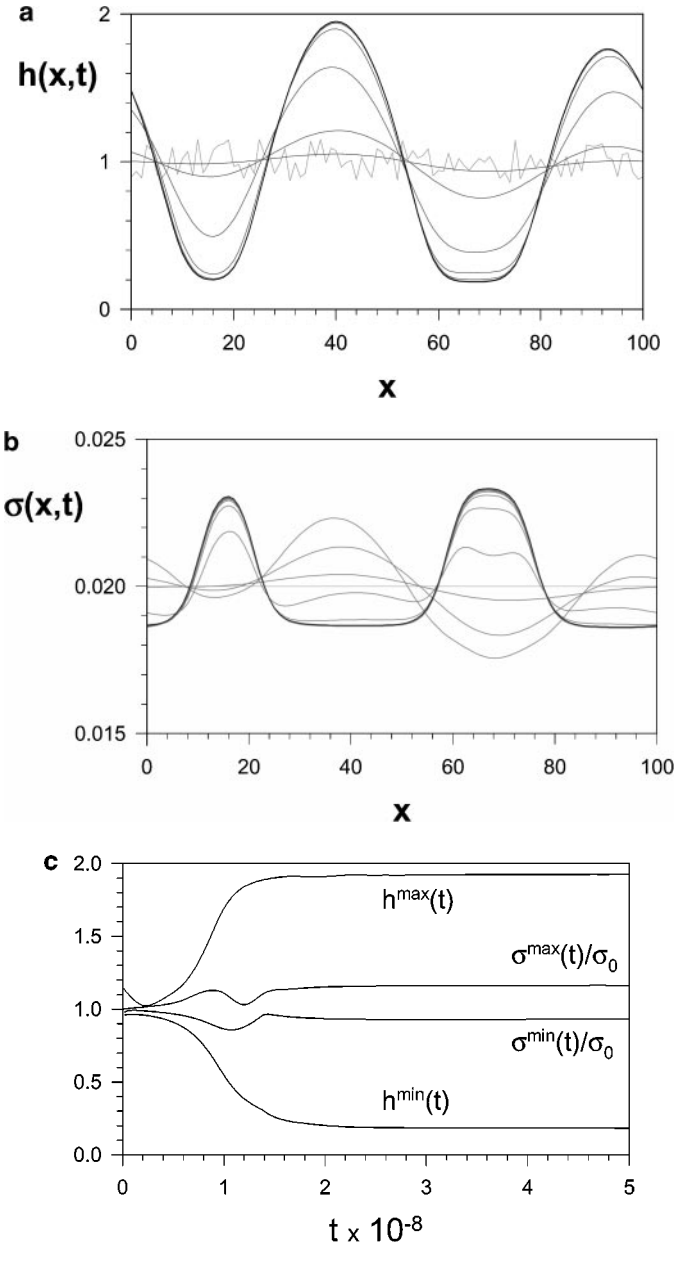

FIG. 4. Shape of the film surface $h(x, t)$ (a) and shape of vesicle charge density profile $\sigma(x, t)$ (b), obtained from numerical integration, as a function of x at various times t, starting from a random initial condition for the film thickness ($\epsilon = 0.15$) and $\sigma_0 = 0.02$ at $t = 0$ (light gray), at intervals of $\Delta t = 4 \times 10^7$ up to $t = 4.8 \times 10^8$ (black). The bounded domain with PBC is taken as $0 \le x \le L$, where $L = 100$. Integration was performed over a grid of 100 cells. (c) The temporal behavior of the minimal and maximal values of $h(x, t)$ and $\sigma(x, t)$ for control stability. Dimensionless parameters are $\sigma_s = -0.04$, $\mu_d = -10$, $\tilde{M} = 10^{-3}$, $\Sigma_0 = 10^{-3}$, $D = 10^{-5}$, and $\kappa = 10/3$.

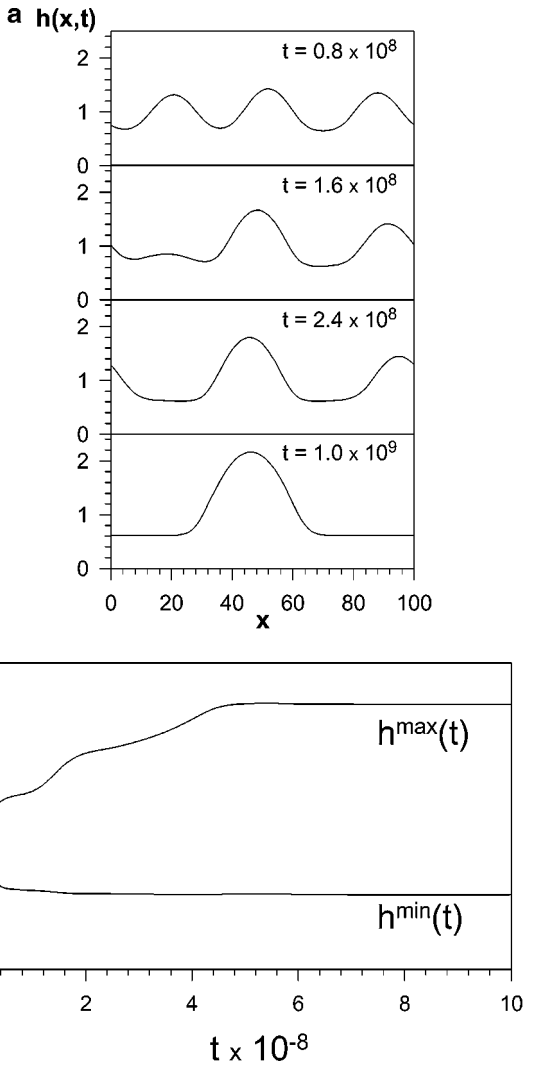

FIG. 5. Multiplicity of the steady state solutions and wavelength selection. (a) Shapes of the film surface $h(x, t)$, obtained from numerical integration, as a function of x at various times t indicated on the figure. All parameters are as in Fig. 4 except for $\sigma_s = -0.15$. (b) The temporal behavior of the minimal and maximal values of $h(x, t)$.

DISCUSSION

The set of Eqs. [1] describes the evolution of a thin liquid film between a substrate and a water–membrane interface with insoluble charged surfactants. It is well established that the requirement for the onset of patterns is the existence of a competition between attractive and repulsive external stresses. If the substrate and the free interface have opposite electric charges, the electric disjoining pressure has attractive and repulsive contributions that make possible the formation of patterns. In fact, patterns for the film thickness, as those observed in phenomena such as charged vesicle blistering, can be predicted by the present model.

Concerning surfactant concentration, it was shown that, in interfaces with one species of neutral surfactant, patterns for the sufactant concentration do not appear although the film

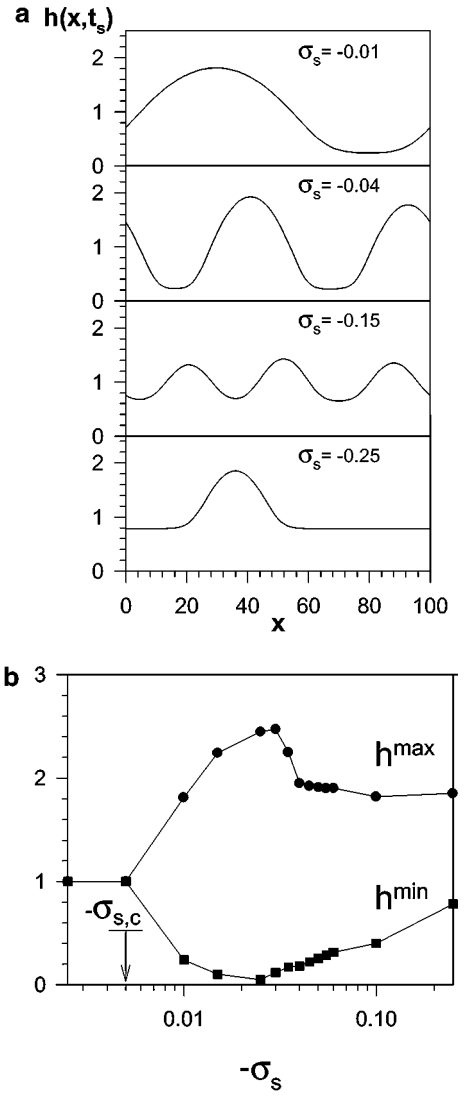

FIG. 6. Profile wavelength and amplitude dependence on the support charge σ_s. (a) Film thickness profiles $h(x, t_s)$ as a function of x at a time t_s belonging to the first plateaux of $h^{\max}(t)$ as in Fig. 5b, for various values of σ_s indicated on the figure. All other parameters as in Fig. 4. (b) Maximal and minimal values of the film thickness at a time t_s as a function of σ_s.

thickness reaches nonhomogeneous steady states. Here, the inclusion of an electrochemical diffusion term in the evolution equation for the surfactant concentration leads to a new outcome concerning pattern formation in thin liquid films, namely, steady patterns for the surfactant concentration (see Fig. 4b). Although charged surfactants in the interface initially move toward the crests, the direction of their movement is further reversed and at last they are more concentrated where the film is narrower. The simple model studied here may improve the understanding on the formation of adhesion plaques of interacting biomembranes in tissue development and immunology (26), where phase separation driven by electrochemical diffusion could play the role of an intermediate pathway followed by specific lock-and-key recognition or by the formation of receptor–ligand pairs.

Unlike the equations derived for a water–gas interface where the gas viscosity is neglected we obtained a system of equations that takes into account the viscosity of the membranous adjacent phase. This viscosity appears in the factor μ_d, the difference between the dimensionless viscosities of the film phase and of the bulk phase, that is related to the Marangoni term. Because the membrane viscosity is higher than that of the water phase, μ_d changes the sign of the Marangoni term.

Our system of two coupled equations could be straightforwardly generalized in order to describe the presence of an arbitrary number, N, of insoluble surfactant species. In the case of N species, a system of $N + 1$ nonlinear coupled equations for the film thickness h and for the concentrations $\Gamma^{(j)}(j = 1, \ldots, N)$ of each insoluble surfactant species will result. Evolution equations are analogous to those derived in the Appendix, but the Marangoni terms are replaced by a sum over all species contributions since the surface tension Σ satisfies the constitutive relation,

$$\Sigma = \Sigma_0 - \sum_{j=1}^{N} M^{(j)}\Gamma^{(j)}, \qquad [12]$$

where $M^{(j)}$ is the Marangoni number associated to the j species. The particular physicochemical parameters (lateral diffusion coefficient, molar electric charge, etc.) of each species should be considered in the evolution equation for the respective concentration. Therefore, the present model could be extended to more general systems where various types of lipids or other surface-active substances are present.

As derived from the linear analysis (Fig. 3b), as well as from numerical simulations (Fig. 6b), the model predicts the existence of a the threshold value $-\sigma_{s,c}$ for the instabilities to appear. This change of behavior is consistent with the experimental observations by Nardi *et al.* (16) who detect two regimes as the charge of the supported membrane increases, one where the vesicle surface is flat and another where patterns of blisters appear. The fact that the critical value increases with σ_0 can also be explained by the model.

The variations of the characteristic wavelengths of the blisters with the substrate and membrane charges are also foreseen by the model. The linear analysis predicts that changing the value of σ_s, the critical wavelength λ_c ($\lambda_c = 2\pi/k_c$), whose variation accompanies that of the fastest growth mode, presents a minimum. This minimum is clearly observed in Fig. 6a, obtained by numerical integration. Numerical results provide additional information such as the minimal thickness and the amplitude of the deformation which is related to the size of the blisters. Figure 6a, is consistent with the growth of the number of blisters in Nardi *et al.* experiments as the support charge increases above the threshold.

It is known that the dewetting of solid surfaces covered by thin liquid films can display several stages, one of them being the coalescence of small holes to form larger dry regions (27). Also, in the electrostatic interaction between a lipid vesicle and

a supported membrane, small blisters collapse into larger ones with the consequent reduction of the number of blisters (16). The mechanism of wavelength selection shown in Fig. 5, which was also observed in the case of thin films bounded by a gas phase (3–6, 9–11), could explain such phenomena.

In the numerical simulations, blisters first appear for a dimensionless time of the order of 10^8 (Fig. 5) that corresponds to a dimensional time of 0.1 s. When comparing that time with experimental ones, one should take into account the size of the system. The larger the system, the larger the time that results from the numerical experiments. In this paper the simulations were carried out for a system 1 μm large ($L = 100$ and $h_0 = 10$ nm).

Following our results, charge separation can be expected (see Fig. 4b) as already conjectured by Nardi *et al.* (16). They concluded from an equilibrium thermodynamic approach that blistering and charge segregation may occur. In their approach the total free energy per unit area takes into account the electrical energy per unit area in the equilibrium state plus the chemical potential associated with the translational entropy of the amphiphiles in the free surface (vesicle). In that case, a criterion of stability was obtained under the assumption that $\sigma_0 \ll -\sigma_s$. On the other hand, our model shows that charge separation and blistering are possible under less restrictive hypothesis concerning the charge densities on the free surface and on the support. The evolution Eq. [1b] for the charge concentration σ, at the stationary state $\sigma_t = 0$, is a complete description of the phase separation due to electrochemical diffusion and mechanical coupling. Beyond the prediction of the onset of instabilities, our dynamical approach provides an understanding of the mechanism of pattern stabilization, namely, external stress and capillary action balance suffices for the onset of nontrivial steady states.

The present model is consistent with experimental observations. Although the resulting equation set is highly nonlinear and a numerical treatment is required for solving it, the linear analysis provides a useful key for predicting the dependence of the blistering phenomenon on the physicochemical parameters involved.

APPENDIX

De Wit and Gallez (20) considered a thin aqueous film under attractive van der Waals bulk forces bounded by a substrate and a nonviscous gaseous phase with one species of (uncharged) surfactant molecules on the water–gas interface. A system of two coupled equations for the film thickness h and for the surfactant concentration Γ was then obtained.

Here, we follow the same steps to derive the evolution equations for a thin aqueous film bounded by a substrate and a viscous fluid layer (membrane) with insoluble surfactants on the water–membrane interface. We also consider the presence of external stresses that generate normal Π and tangential τ stresses on the interfaces as well as a conservative body force with potential Φ.

In order to apply lubrication theory, the Navier–Stokes and continuity equations together with the boundary conditions are set in a dimensionless form. Dimensionless variables are introduced via length $\bar{h}_0$, and time $\bar{h}_0^2/\bar{\nu}$. A second scaling is further carried out by defining the small parameter $\eta = \bar{h}/\bar{\lambda} \ll 1$, where $\bar{\lambda}$ is the wavelength of the deformation. The total scaling on the spatial and temporal variables reads

$$\begin{aligned} x &= \eta(1/\bar{h}_0)\bar{x}, \qquad z = (1/\bar{h}_0)\bar{z}, \\ h &= (1/\bar{h}_0)\bar{h}, \qquad t = \eta^n\left(\bar{\nu}/\bar{h}_0^2\right)\bar{t}, \end{aligned} \tag{A-1}$$

where the rescaled variables are all unit order as $\eta \to 0$ and the integer $n \geq 2$ will be fixed in order to define a time scale compatible with the diffusion rate of the surfactant molecules.

The tangential u and normal w components of the two-dimensional velocity field are then given by

$$u = \eta^{1-n}(\bar{h}_0/\bar{\nu})\bar{u}, \qquad w = \eta^{-n}(\bar{h}_0/\bar{\nu})\bar{w}, \tag{A-2}$$

while the mechanical pressures $\bar{p}$ and $\bar{p}'$, inside the aqueous film and the membrane, respectively, are rescaled as

$$p = \eta^{n-2}\left(\bar{h}_0^2/\bar{\rho}\,\bar{\nu}^2\right)\bar{p}, \qquad p' = \eta^{n-1}\left(\bar{h}_0^2/\bar{\rho}\bar{\nu}^2\right)\bar{p}'. \tag{A-3}$$

Approximate solutions of the rescaled problem can be obtained by introducing the following regular perturbation expansion:

$$(u, w, p, p') = \sum_{i\geq 0} \eta^i (u_i, w_i, p_i, p_i'). \tag{A-4}$$

The set of evolution equations for a film on a solid substrate can be obtained from the zeroth-order problem (De Wit and Gallez 1994). Hence, from now on, we will consider the zeroth-order governing equations and boundary conditions (with the "0" subscripts omitted) for the thin aqueous film. At zeroth-order, the x- and z-components of the Navier–Stokes equations are

$$(p + \Phi)_x = u_{zz}, \tag{A-5}$$

$$(p + \Phi)_z = 0, \tag{A-6}$$

where the potential $\bar{\Phi}$ is rescaled as

$$\Phi = \eta^{n-2}\left(\bar{h}_0^2/\bar{\rho}\bar{\nu}^2\right)\bar{\Phi}, \tag{A-7}$$

and the continuity equation reads

$$u_x + w_z = 0. \tag{A-8}$$

We assume no-slip and no-penetration conditions on the substrate, i.e.,

$$u = 0, \qquad w = 0, \qquad \text{[A-9]}$$

as well as the continuity of the velocity through the free surface.

The normal and tangential stress balances on the water-membrane interface ($z = h$) at zeroth-order read, respectively,

$$p + \Pi = -\Sigma_0 h_{xx}, \qquad \text{[A-10]}$$

and

$$\mu_d u_z = -M\Gamma_x + \tau, \qquad \text{[A-11]}$$

with

$$\mu_d = 1 - \mu'/\mu. \qquad \text{[A-12]}$$

In Eq. [A-10] the normal stress Π is taken as

$$\Pi = \eta^{n-2}\left(\bar{h}_0^2/\overline{\rho v^2}\right)\bar{\Pi}. \qquad \text{[A-13]}$$

Note that the term containing p' does not appear as a consequence of the scalings in Eq. [A-3] which are reasonable whenever $\Pi < 0$.

In Eq. [A-11], M is the Marangoni number and we have supposed that

$$M\Gamma = \eta^{n-2}(\bar{h}_0/\bar{\rho}\,\bar{v}^2)\bar{M}\bar{\Gamma}. \qquad \text{[A-14]}$$

The shear stress (Eq. [A-11]) is taken as

$$\tau = \eta^{n-1}\left(\bar{h}_0^2/\overline{\rho v^2}\right)\bar{\tau}. \qquad \text{[A-15]}$$

The surface tension Σ was defined by the following constitutive relation:

$$\Sigma = \Sigma_0 - M\Gamma. \qquad \text{[A-16]}$$

The kinematic boundary condition at $z = h(x, t)$ is given by

$$w = h_t + uh_x. \qquad \text{[A-17]}$$

The surfactant concentration satisfies the conservation equation

$$\Gamma_t + (\Gamma u)_x = -\nabla \cdot J, \qquad \text{[A-18]}$$

where J is the dimensionless surface flux. In an ideal ionic solution J will be given by minus the gradient of the electrochemical potential that satisfies

$$\nabla \cdot J = -D(\Gamma_x + \tilde{Z}\Gamma\psi_x)_x, \qquad \text{[A-19]}$$

where, D is the lateral diffusion coefficient and ψ is the electric surface potential.

A straightforward integration of the above Navier–Stokes and continuity equations with the associated boundary conditions leads to the following system of evolution equations for the film thickness h and surfactant concentration Γ:

$$h_t = \left[\frac{h^2}{2}\left(\frac{M}{\mu_d}\Gamma_x - \tau\right) - \frac{\Sigma_0}{3}h^3 h_{xxx} - \frac{h^3}{3}(\Phi - \Pi)_x\right]_x,$$

$$\Gamma_t = -\nabla \cdot J + \left[h\left(\frac{M}{\mu_d}\Gamma_x - \tau\right) - \frac{\Sigma_0}{2}h^2\Gamma h_{xxx} - \frac{h^2}{2}\Gamma(\Phi - \Pi)_x\right]_x. \qquad \text{[A-20]}$$

ACKNOWLEDGMENTS

We acknowledge Brazilian Agencies, CNPq, Capes, and FAPERJ for partial financial support.

REFERENCES

1. Oron, A., Davis, S. H., and Bankoff, S. G., Long-scale evolution of thin liquid films. *Rev. Mod. Phys.* **69**(3), 931–980 (1997).
2. Sharma, A., Relationship of thin-film stability and morphology to macroscopic parameters of wetting in the apolar and polar systems. *Langmuir* **9**(3), 861–869 (1993).
3. Sharma, A., and Jammel, A., Nonlinear stability, rupture and morphological phase separation of thin fluid films on apolar and polar substrates. *J. Colloid Interface Sci.* **161,** 190–208 (1993).
4. Jameel, A. T., and Sharma, A., Morphological phase separation in thin liquid filmes. II. Equilibrium contact angles of nanodrops coexisting with films. *J. Colloid Interface Sci.* **164,** 416–427 (1994).
5. Mitlin, V. S., Dewetting of solid surface: Analogy with spinodal decomposition. *J. Colloid Interface Sci.* **156,** 491–497 (1993).
6. Mitlin, V. S., and Petviashvili, N. V., Nonlinear dynamics of dewetting: Kinetically stable structures. *Phys. Lett. A* **192,** 323–326 (1994).
7. Ramos de Souza, E., Anteneodo, C., Costa Pinto, N. M., and Bisch, P. M., Nonlinear dynamics of lipid films under electric forces. *J. Colloid Interface Sci.* **187,** 313–326 (1997).
8. Erneux, T., and Gallez, D., Can repulsive forces lead to stable patterns in thin liquid films? *Phys. Fluids* **9**(4), 1194–1196 (1997).
9. Sharma, A., and Khanna, R., Pattern formation in unstable thin liquid films. *Phys. Rev. Lett.* **81**(16), 3463–3466 (1998).
10. Sharma, A., and Khanna, R., Self-organization in thin liquid films dynamics and patterns in systems displaying a secondary minimum. *J. Adhesnol. Tech.* **14,** 145–166 (2000).
11. Ramos de Souza, E., and Gallez, D., Pattern formation in thin liquid films with insoluble surfactants. *Phys. Fluids* **10,** 1804–1814 (1998).
12. Sackmann, E., Supported membranes: Scientific and practical applications. *Science* **271,** 43–49 (1996).
13. Gallez, D., and Coakley, W. T., Far-from-equilibrium phenomena in bioadhesion processes. *Heterog. Chem. Rev.* **3,** 443–449 (1996).
14. Coakley, W. T., Gallez, D., Ramos de Souza, E., and Gauci, H., Ionic strength dependence of localized contact formation between membranes. *Biophys. J.* **77,** 817–828 (1999).
15. Evans, E., Physical action in biological adhesion, *in* "Handbook of Biological Physics" (R. Lipowsky and E. Sackmann, Eds.), Vol. 1, pp. 723–754. Elsevier, Amsterdam, 1995.

16. Nardi, J., Feder, T., Bruinsma, R., and Sackmann, E., Electrostatic adhesion between fluid membranes: Phase separation and blistering. *Europhys. Lett.* **37**(5), 371–376 (1997).
17. Nardi, J., Feder, T., Bruinsma, R., and Sackmann, E., Adhesion-induced reorganisation of charged fluid membranes. *Phys. Rev. E* **58**(5), 6340–6354 (1998).
18. Pantazatos, D. P., and MacDonald, R. C., Directly observed membrane fusion between oppositely charged phospholipid bilayers. *Membrane Biol.* **170,** 27–38 (1999).
19. Parsegian, V. A., and Gingell, D., On the electrostatic interaction across a salt solution between two bodies bearing unequal charges. *Biophys. J.* **12,** 1192–1204 (1972).
20. De Wit, A., Gallez, D., and Christov, I., Nonlinear evolution equations for thin liquid films with insoluble surfactants. *Phys. Fluids* **6**(10), 3256–3266 (1994).
21. Sternling, C. V., and Scriven, L. E., Interfacial turbulence: Hydrodynamic instability and the Marangoni effect. *AIChE J.* **5**(4), 514–523 (1959).
22. Williams, M. B., and Davis, S. H., Nonlinear theory of film rupture. *J. Colloid Interface Sci.* **90**(1), 220–228 (1982).
23. Verwey, E. J. W., and Overbeek, J. Th. G., "Theory of the Stability of Lyophobic Colloids/The Interaction of Sol Particles having an Electric Double Layer." Elsevier, New York, 1948.
24. Bisch, P. M., and Wendel, H., Remark on disjoining pressure in free liquid films. *J. Colloid Interface Sci.* **96**(2), 555–557 (1983).
25. Press, W. H., Flannery, B. P., Teukolsky, S. A., and Vetterling. W. T., "Numeric Recipes. The Art of Scientific Computing," Cambridge University Press, Cambridge, 1986.
26. Alberts, B., Bray, D., Lewis, J., Raff, M., Roberts, K., and Watson. J. D., "Molecular Biology of The Cell," 3rd ed., Garland Publishing, New York, 1994.
27. Sharma, A., and Reiter, G., Instability of thin polymer films on coated substrates: Rupture, dewetting, and drop formation. *J. Colloid Interface Sci.* **178,** 243–268 (1996).